
Generalizing Point Embeddings using the Wasserstein Space of Elliptical Distributions

Boris Muzellec
 CREST, ENSAE
 Université Paris-Saclay
 boris.muzellec@ensae.fr

Marco Cuturi
 CREST, ENSAE
 Université Paris-Saclay
 marco.cuturi@ensae.fr

Abstract

Embedding complex objects as vectors in low dimensional spaces is a longstanding problem in machine learning. We propose in this work an extension of that approach, which consists in embedding objects as elliptical probability distributions, namely distributions whose densities have elliptical level sets. We endow these measures with the 2-Wasserstein metric, with two important benefits: (i) For such measures, the squared 2-Wasserstein metric has a closed form, equal to the sum of the squared Euclidean distance between means and the squared Bures metric between covariance matrices. The latter is a Riemannian metric between positive semi-definite matrices, which turns out to be Euclidean on a suitable factor representation of such matrices, which is valid on the entire geodesic between these matrices. (ii) The 2-Wasserstein distance boils down to the usual Euclidean metric when comparing Diracs, and therefore provides the natural framework to extend point embeddings. We show that for these reasons Wasserstein elliptical embeddings are more intuitive and yield tools that are better behaved numerically than the alternative choice of Gaussian embeddings with the Kullback-Leibler divergence. In particular, and unlike previous work based on the KL geometry, we learn elliptical distributions that are not necessarily diagonal. We demonstrate the interest of elliptical embeddings by using them for visualization, to compute embeddings of words, and to reflect entanglement or hypernymy.

1 Introduction

One of the holy grails of machine learning is to compute meaningful low-dimensional embeddings for high-dimensional complex objects. That ability is crucial to tackle advanced tasks, such as inference on texts using word embeddings [Pennington et al., 2014, Bojanowski et al., 2016], image understanding [Norouzi et al., 2014] or concise representations for nodes in a huge graph [Grover and Leskovec, 2016]. When those embeddings are extremely small (2 or 3 numbers) they can also be used for data visualization.

Early references in this field focused on creating *isometric* embeddings in target low dimensional Euclidean spaces $\mathcal{Y} = \mathbb{R}^d$, building upon strong mathematical foundations [Bourgain, 1985, Johnson and Lindenstrauss, 1984]. Given input points x_1, \dots, x_n , the goal was to compute embeddings $\mathbf{y}_1, \dots, \mathbf{y}_n$ in \mathbb{R}^d whose pairwise distances $\|\mathbf{y}_i - \mathbf{y}_j\|_2$ would not depart from the original distances $d_{\mathcal{X}}(x_i, x_j)$. Starting with metric multidimensional scaling (mMDS) [De Leeuw, 1977, Borg and Groenen, 2005], several approaches have refined this intuition [Tenenbaum et al., 2000, Roweis and Saul, 2000, Hinton and Roweis, 2003, Maaten and Hinton, 2008]. More general criteria, such as reconstruction error [Hinton and Salakhutdinov, 2006, Kingma and Welling, 2013], co-occurrence [Globerson et al., 2007], or relational knowledge, be it in metric learning [Weinberger and Saul, 2009] or for word embeddings [Mikolov et al., 2013b] can be used to obtain vector embeddings,

whose distance or more generally dot-products $\langle \mathbf{y}_i, \mathbf{y}_j \rangle$ must comply with some desiderata. More general and flexible approaches in which the embedding space \mathcal{Y} needs not be Euclidean have also been considered, for instance in generalized MDS on the sphere [Maron et al., 2010], on surfaces [Bronstein et al., 2006], in spaces of trees [Bădoiu et al., 2007, Fakcharoenphol et al., 2003], or, more recently computed in the Poincaré hyperbolic space [Nickel and Kiela, 2017].

Probabilistic Embeddings Our work belongs to a recent trend, pioneered by Vilnis and McCallum, who proposed to embed data points as *probability measures* in \mathbb{R}^d [2015]. Usual point embeddings can be regarded as a very particular and degenerate case of probability measures, in which the mass is infinitely concentrated on a single point (a Dirac). Probability measures that are more spread-out, or even multimodal, provide therefore additional flexibility. To exploit this, Vilnis and McCallum proposed to embed words as *Gaussians* endowed with the Kullback-Leibler (KL) divergence or the usual ℓ_2 metric [Smola et al., 2007]. Athiwaratkun and Wilson have extended the latter approach to mixtures of Gaussians [2017]. The Kullback-Leibler and ℓ_2 geometries on measures have, however, an important drawback: these geometries do not coincide with the usual Euclidean metric between point embeddings when the variances of these Gaussians collapse and become diracs. Indeed, the KL divergence between two Gaussians diverges to ∞ when their variances become small, whereas the ℓ_2 distance saturates and becomes 1 no matter where the Gaussians are located. Numerical issues arising from these degeneracies are avoided in these works by often times switching back to a simple Euclidean metric at test time (see our comments in Table 1).

Contributions We propose in this work a comprehensive framework for probabilistic embeddings, in which point embeddings are seamlessly handled as a particular case. We consider arbitrary families of elliptical distributions, not necessarily Gaussians, and focus in particular on uniform elliptical distributions, that are more intuitive to handle because of their compact support. The cornerstone of our approach lies in the use of the 2-Wasserstein distance, which can handle degenerate measures and admits a closed form, both for the metric and its gradient [Gelbrich, 1990] in its original Riemannian formulation and more amenable Euclidean parameterization. We provide numerical tools to carry out the computation of embeddings in different scenarii, both to optimize with respect to the metric as is done in multidimensional scaling, or with respect to a dot-product, as shown in our applications to word embeddings for entailment, similarity and hypernymy tasks.

Notations \mathcal{S}_{++}^d (resp. \mathcal{S}_+^d) is the set of positive (resp. semi-)definite $d \times d$ matrices. For two vectors $\mathbf{x}, \mathbf{y} \in \mathbb{R}^d$ and a matrix $\mathbf{M} \in \mathcal{S}_+^d$, we write the Mahalanobis norm induced by \mathbf{M} as $\|\mathbf{x} - \mathbf{c}\|_{\mathbf{M}}^2 = (\mathbf{x} - \mathbf{c})^T \mathbf{M} (\mathbf{x} - \mathbf{c})$ and $|\mathbf{M}|$ for $\det(\mathbf{M})$. For V an affine subspace of dimension m in \mathbb{R}^d , λ_V is the Lebesgue measure on that subspace. M^\dagger is the pseudo inverse of M .

2 The Geometry of Elliptical Distributions in the Wasserstein Space

We recall in this section basic facts about elliptical distributions in \mathbb{R}^d . We adopt a general formulation that includes measures supported on subspaces of \mathbb{R}^d and Dirac (point) measures. That level of generality is needed to provide a seamless connection with usual vector embeddings, seen in our context as Dirac masses. We follow with the definition of the 2-Wasserstein distance between two distributions from a given elliptical family.

Elliptically Contoured Densities In their simplest form, elliptical distributions can be seen as generalizations of Gaussian multivariate densities in \mathbb{R}^d : their level sets describe concentric ellipsoids, shaped following a scale parameter $\mathbf{C} \in \mathcal{S}_{++}^d$ and centered around a mean parameter $\mathbf{c} \in \mathbb{R}^d$ [Cambanis et al., 1981]. The density at a point \mathbf{x} of such distributions is $h(\|\mathbf{x} - \mathbf{c}\|_{\mathbf{C}^{-1}}) / \sqrt{|\mathbf{C}|}$ where the generator function h is such that $\int_{\mathbb{R}^d} h(\|\mathbf{x}\|^2) d\mathbf{x} = 1$. Gaussians are recovered with $h = g, g(\cdot) \propto e^{-\cdot/2}$ while uniform distributions on full rank ellipsoids result from $h = u, u(\cdot) \propto \mathbf{1}_{\leq 1}$.

Because the norm induced by \mathbf{C}^{-1} appears in formulas above, the scale parameter \mathbf{C} must have full rank for these definitions to be meaningful. Cases where \mathbf{C} does not have full rank can appear when a probability measure is supported on an affine subspace of \mathbb{R}^d , such as lines in \mathbb{R}^2 or even possibly a space of null dimension when the measure is supported on a single point (a Dirac measure).

Elliptical Distributions To lift this limitation, several reformulations of elliptical distributions have been proposed to handle degenerate scale matrices \mathbf{C} of rank $\text{rk } \mathbf{C} < d$. A first approach is given by a parameterization of these distributions through their characteristic function [Cambanis et al., 1981,

Fang et al., 1990]. In a nutshell, recall that the characteristic function of a multivariate Gaussian is equal to $\phi(\mathbf{t}) = e^{i\mathbf{t}^T \mathbf{c}} g(\mathbf{t}^T \mathbf{C} \mathbf{t})$ where $g(\cdot) = e^{-\cdot/2}$. A natural generalization is to consider for g other functions of positive type [Ushakov, 1999, Theo.1.8.9] of the argument $\mathbf{t}^T \mathbf{C} \mathbf{t}$. This parameterization does not require the scale parameter \mathbf{C} to be invertible. The second approach is that taken by Gelbrich [1990, Theorem 2.4], upon which most of this work is grounded. His definition of (possibly degenerate) elliptical distributions casts them as measures that have a density with respect to the Lebesgue measure of dimension $\text{rk } \mathbf{C}$, in the affine space $\mathbf{c} + \text{Im } \mathbf{C}$, where the image of \mathbf{C} is $\text{Im } \mathbf{C} \stackrel{\text{def}}{=} \{\mathbf{C}\mathbf{x}, \mathbf{x} \in \mathbb{R}^d\}$.

Both constructions are relatively complex, and we refer the interested reader to these references for a rigorous treatment. For the purpose of this work, we will focus on two important results on these distributions: their variance can be computed as a multiple of their scale parameter \mathbf{C} , and their 2-Wasserstein distance has a closed form.

Rank Deficient Uniform Elliptical Distributions and their Variances Because they are easier to visualize, we consider in the following compactly supported *uniform* elliptical distributions. Consider a mean vector $\mathbf{c} \in \mathbb{R}^d$, and a scale *semi*-definite matrix $\mathbf{C} \in S_+^d$. Let $\mu_{\mathbf{c}, \mathbf{C}}$ be the *uniform* measure on the affine space $\mathbf{c} + \text{Im } \mathbf{C}$ with support $\{\mathbf{c} + \mathbf{C}^{1/2} \mathbf{y} : \mathbf{y} \in \mathbb{R}^d, \|\mathbf{y}\|^2 \leq 1\}$. Examples of such uniform elliptical distributions, including a Dirac ($\mathbf{C} = \mathbf{0}$), are displayed in Figure 1.

Let \mathcal{P}_u be the set of uniform elliptical measures, $\mathcal{P}_u = \{\mu_{\mathbf{c}, \mathbf{C}}, \mathbf{c} \in \mathbb{R}^d, \mathbf{C} \in S_+^d\}$. For such measures, one can prove [Gelbrich, 1990, p.195] that their covariance matrix is *proportional* to their scale parameter, namely

$$\text{var}(\mu_{\mathbf{c}, \mathbf{C}}) = \frac{1}{d+2} \mathbf{C}. \quad (1)$$

That link between scale and covariance matrices is not limited to uniform measures (for Gaussians, they coincide) and applies to any family of elliptical distributions, through a constant τ_h that depends on the generator function h . Here, $\tau_u = 1/(d+2)$ and $\tau_g = 1$.

The 2-Wasserstein Bures Metric A natural metric for elliptical distributions arises from optimal transport (OT) theory. We refer the interested reader to [Santambrogio, 2015] for an exhaustive survey on OT. Recall that for two arbitrary probability measures $\mu, \nu \in \mathcal{P}(\mathbb{R}^d)$, their squared 2-Wasserstein distance is equal to

$$W_2^2(\mu, \nu) \stackrel{\text{def}}{=} \inf_{X \sim \mu, Y \sim \nu} \mathbb{E} \|X - Y\|_2^2.$$

This formula rarely has a closed form. However, in the footsteps of Dowson and Landau [1982] who proved it for Gaussians, Gelbrich [1990] has shown that for two distributions $\alpha \stackrel{\text{def}}{=} \mu_{\mathbf{a}, \mathbf{A}}$ and $\beta \stackrel{\text{def}}{=} \mu_{\mathbf{b}, \mathbf{B}}$ in \mathcal{P}_u , one has

$$W_2^2(\alpha, \beta) = \|\mathbf{a} - \mathbf{b}\|_2^2 + \mathfrak{B}^2(\text{var } \alpha, \text{var } \beta) = \|\mathbf{a} - \mathbf{b}\|_2^2 + \frac{1}{d+2} \mathfrak{B}^2(\mathbf{A}, \mathbf{B}), \quad (2)$$

where \mathfrak{B}^2 is the (squared) Bures metric on S_+^d , proposed in quantum information geometry [1969] and studied recently in [Bhatia et al., 2018, Malagò et al., 2018],

$$\mathfrak{B}^2(\mathbf{X}, \mathbf{Y}) \stackrel{\text{def}}{=} \text{Tr}(\mathbf{X} + \mathbf{Y} - 2(\mathbf{X}^{\frac{1}{2}} \mathbf{Y} \mathbf{X}^{\frac{1}{2}})^{\frac{1}{2}}). \quad (3)$$

The factor $1/(d+2)$ in front of the rightmost term \mathfrak{B}^2 in (2) arises from homogeneity of \mathfrak{B}^2 in its arguments (3), and the identity in (1).

A few remarks (i) When both scale matrices $\mathbf{A} = \text{diag } \mathbf{d}_\mathbf{A}$ and $\mathbf{B} = \text{diag } \mathbf{d}_\mathbf{B}$ are diagonal, $W_2^2(\alpha, \beta)$ is the sum of two terms: the usual squared Euclidean distance between their means, plus

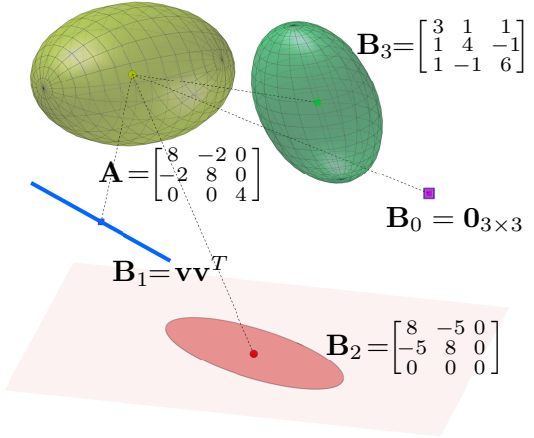


Figure 1: Five measures from the family of uniform elliptical distributions in \mathbb{R}^3 . Each measure has a mean (location) and scale parameter. In this carefully selected example, the reference measure (with scale parameter \mathbf{A}) is equidistant (according to the 2-Wasserstein metric) to the four remaining measures, whose scale parameters $\mathbf{B}_0, \mathbf{B}_1, \mathbf{B}_2, \mathbf{B}_3$ have ranks equal to their indices (here, $\mathbf{v} = [3, 7, -2]^T$).

$1/(d+2)$ times the squared *Hellinger* metric between the diagonals $\mathbf{d}_A, \mathbf{d}_B$, $\mathfrak{H}^2(\mathbf{d}_A, \mathbf{d}_B) \stackrel{\text{def}}{=} \|\sqrt{\mathbf{d}_A} - \sqrt{\mathbf{d}_B}\|_2^2$. (ii) The distance W_2 between two Diracs δ_a, δ_b is equal to the usual distance between vectors $\|\mathbf{a} - \mathbf{b}\|_2$. (iii) The squared distance W_2^2 between a Dirac δ_a and a measure $\mu_{\mathbf{b}, \mathbf{B}}$ in \mathcal{P}_u reduces to $\|\mathbf{a} - \mathbf{B}\|^2 + \text{Tr} \mathbf{C} / (d+2)$. The distance between a point and a uniform ellipsoid therefore always *increases* as the scale parameter of the latter increases. Although this point makes sense from the quadratic viewpoint of W_2^2 (in which the quadratic contribution $\|\mathbf{a} - \mathbf{x}\|_2^2$ of points \mathbf{x} in the ellipsoid that stand further away from \mathbf{a} than \mathbf{b} will dominate that brought by points \mathbf{x} that are closer, see Figure 3) this may be counterintuitive for applications to visualization, an issue that will be addressed in Section 4. (iv) The W_2 distance between two uniform elliptical distributions is always finite, no matter how degenerate they are. This is illustrated in Figure 1 in which a 3D measure $\mu_{\mathbf{a}, \mathbf{A}}$ is shown to be exactly equidistant to four other measures, some of which are degenerate. However, as can be hinted by the simple example of the Hellinger metric, that distance may not be differentiable for degenerate measures (in the same sense that $(\sqrt{x} - \sqrt{y})^2$ is defined at $x = 0$ but not differentiable w.r.t x).

3 Optimizing over the Space of Elliptical Embeddings

Our end goal is to use the space of elliptical distributions as an embedding space. The optimization of such embeddings will rely on their relative W_2 distances. To optimize loss functions involving W_2 terms, we need suitable parameterizations of these embeddings. Mean parameters are simple vectors in \mathbb{R}^d and only appear in the computation of W_2 through their Euclidean metric, they are therefore not a concern and can be addressed with standard tools. Scale parameters are, on the contrary, constrained to lie in S_+^d . Rather than updating them, we advocate optimizing directly on factors of such parameters, which results in simple Euclidean (unconstrained) updates.

Geodesics for Elliptical Distributions When \mathbf{A} and \mathbf{B} have full rank, the geodesic from α to β is a curve of measures in the same family of elliptic distributions, characterized by location and scale parameters $\mathbf{c}(t), \mathbf{C}(t)$, where

$$\mathbf{c}(t) = (1-t)\mathbf{a} + t\mathbf{b}; \quad \mathbf{C}(t) = ((1-t)\mathbf{I} + t\mathbf{T}^{\mathbf{AB}}) \mathbf{A} ((1-t)\mathbf{I} + t\mathbf{T}^{\mathbf{AB}}) \quad (4)$$

and matrix $\mathbf{T}^{\mathbf{AB}}$ is such that $\mathbf{x} \rightarrow \mathbf{T}^{\mathbf{AB}}\mathbf{x}$ is the so-called Brenier optimal transportation map [1987] from α to β ,

$$\mathbf{T}^{\mathbf{AB}} \stackrel{\text{def}}{=} \mathbf{A}^{-\frac{1}{2}} (\mathbf{A}^{\frac{1}{2}} \mathbf{B} \mathbf{A}^{\frac{1}{2}})^{\frac{1}{2}} \mathbf{A}^{-\frac{1}{2}},$$

namely the unique matrix such that $\mathbf{B} = \mathbf{T}^{\mathbf{AB}} \mathbf{A} \mathbf{T}^{\mathbf{AB}}$ ([Peyré and Cuturi, 2018, Remark 2.30]). When \mathbf{A} is degenerate, such a curve still exists as long as $\text{Im } \mathbf{B} \subset \text{Im } \mathbf{A}$, in which case the expression above is still valid using pseudo-inverse square roots $\mathbf{A}^{\dagger/2}$ in place of the usual inverse-square root.

Differentiability in Riemannian Parameterization Scale parameters are, on the contrary restricted to lie on the cone S_+^d . For such problems, it is well known that a direct gradient-and-project based optimization on scale parameters would prove to expensive. A natural remedy to this issue is to perform manifold optimization [Absil et al., 2009]. Indeed, as in any Riemannian manifold, the Riemannian gradient $\text{grad}_x \frac{1}{2} d^2(x, y)$ is given by $-\log_x y$ [Lee, 1997]. Using the expressions of the exp and log given in [Malagò et al., 2018], we can show that minimizing $\frac{1}{2} \mathfrak{B}^2(\mathbf{A}, \mathbf{B})$ using Riemannian gradient descent corresponds to making updates of the form, with step length η

$$\mathbf{A}' = ((1-\eta)\mathbf{I} + \eta\mathbf{T}^{\mathbf{AB}}) \mathbf{A} ((1-\eta)\mathbf{I} + \eta\mathbf{T}^{\mathbf{AB}}) \quad (5)$$

When $0 \leq \eta \leq 1$, this corresponds to considering a new point \mathbf{A}' closer to \mathbf{B} along the Bures geodesic between \mathbf{A} and \mathbf{B} . When η is negative or larger than 1, \mathbf{A}' no longer lies on this geodesic but is guaranteed to remain PSD, as can be seen from (5). Figure 2 shows a W_2 geodesic between two measures μ_0 and μ_1 , as well as its extrapolation following exactly the formula given in (4). That figure illustrates that μ_t is not necessarily geodesic outside of the boundaries $[0, 1]$ w.r.t to three relevant measures, because its metric derivative is smaller than 1 [Ambrosio et al., 2006, Theorem 1.1.2]. When negative steps are taken (for instance when the W_2^2 distance needs to be increased), this lack of geodesicity has proved difficult to handle numerically for a simple reason: such updates may lead to degenerate scale parameters \mathbf{A}' , as illustrated around time $t = 1.5$ of the curve in Figure 2. Another obvious drawback of Riemannian approaches is that they are not as well studied as simpler non-constrained Euclidean problems, for which a plethora of optimization techniques are available. This observations motivates an alternative Euclidean parameterization, explored next.

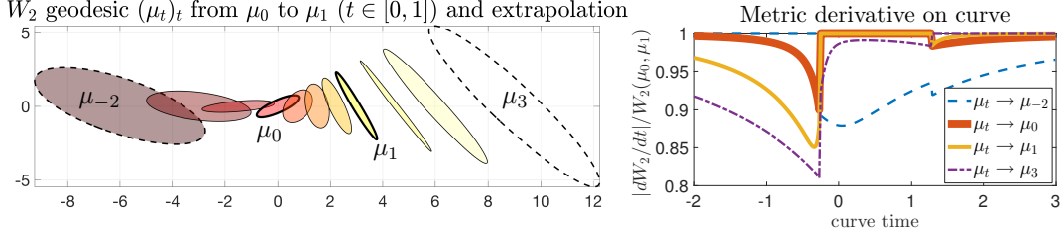


Figure 2: (left) Interpolation $(\mu_t)_t$ between two measures μ_0 and μ_1 following the geodesic equation (4). The same formula can be used to interpolate on the left and right of times 0, 1. Displayed times are $[-2, -1, -.5, 0, .25, .5, .75, 1, 1.5, 2, 3]$. Note that geodesicity is not ensured outside of the boundaries $[0, 1]$. This is illustrated in the right plot displaying normalized metric derivatives of the curve μ_t to four relevant points: $\mu_0, \mu_1, \mu_{-2}, \mu_3$. The curve μ_t is not always locally geodesic, as can be seen by the fact that the metric derivative is strictly smaller than 1 in several cases.

Differentiability in Euclidean Parameterization A canonical way to handle a PSD constraint for \mathbf{A} is to rewrite it in factor form $\mathbf{A} = \mathbf{L}\mathbf{L}^T$. In the particular case of the Bures metric, we show that this simple parametrization comes without losing the geometric interest of manifold optimization, while benefiting from simpler additive updates. Indeed, one can (see supplementary) that the gradient of the squared Bures metric has the following gradient:

$$\nabla_{\mathbf{L}} \frac{1}{2} \mathfrak{B}^2(\mathbf{A}, \mathbf{B}) = (\mathbf{I} - \mathbf{T}^{\mathbf{AB}}) \mathbf{L}, \quad \text{with updates } \mathbf{L}' = ((1 - \eta)\mathbf{I} + \eta \mathbf{T}^{\mathbf{AB}}) \mathbf{L}. \quad (6)$$

Links between Euclidean and Riemannian Parameterization The factor updates in (6) are exactly equivalent to the Riemannian ones (5) in the sense that $\mathbf{A}' = \mathbf{L}'\mathbf{L}'^T$. Therefore, by using a factor parameterization we carry out updates that stay on the Riemannian geodesic yet only require linear updates on \mathbf{L} , independently of the factor \mathbf{L} chosen to represent \mathbf{A} (given a factor \mathbf{L} of \mathbf{A} , any right-side multiplication of that matrix by a unitary matrix remains a factor of \mathbf{A}).

When considering general loss functions \mathcal{L} that take as arguments squared Bures distances, one can also show that \mathcal{L} is geodesically convex w.r.t. to scale matrices \mathbf{A} if and only if it is convex in the usual sense with respect to \mathbf{L} , where $\mathbf{A} = \mathbf{L}\mathbf{L}^T$. Write now $\mathbf{L}_{\mathbf{B}} = \mathbf{T}^{\mathbf{AB}}\mathbf{L}$. One can recover that $\mathbf{L}_{\mathbf{B}}\mathbf{L}_{\mathbf{B}}^T = \mathbf{B}$. Therefore, expanding the expression \mathfrak{B}^2 for the right term below we obtain

$$\mathfrak{B}^2(\mathbf{A}, \mathbf{B}) = \mathfrak{B}^2(\mathbf{L}\mathbf{L}^T, \mathbf{L}_{\mathbf{B}}\mathbf{L}_{\mathbf{B}}^T) = \mathfrak{B}^2(\mathbf{L}\mathbf{L}^T, \mathbf{T}^{\mathbf{AB}}\mathbf{L}(\mathbf{T}^{\mathbf{AB}}\mathbf{L})^T) = \|\mathbf{L} - \mathbf{T}^{\mathbf{AB}}\mathbf{L}\|_F^2$$

Indeed, the Bures distance simply reduces to the Frobenius distance between two factors of \mathbf{A} and \mathbf{B} . However these factors need to be carefully chosen: given \mathbf{L} for \mathbf{A} , the factor for \mathbf{B} must be computed according to an optimal transport map $\mathbf{T}^{\mathbf{AB}}$.

Polarization between Elliptical Distributions Some of the applications we consider, such as the estimation of word embeddings, are inherently based on dot-products. We use the polarization identity to define a “Bures dot-product”, where $\delta_0 = \mu_{0_d, 0_{d \times d}}$ is simply the Dirac mass at $\mathbf{0}$.

$$[\mu_{\mathbf{a}, \mathbf{A}}, \mu_{\mathbf{b}, \mathbf{B}}]_{\mathfrak{B}} \stackrel{\text{def}}{=} \frac{1}{2} (W_2^2(\mu_{\mathbf{a}, \mathbf{A}}, \delta_0) + W_2^2(\mu_{\mathbf{b}, \mathbf{B}}, \delta_0) - W_2^2(\mu_{\mathbf{a}, \mathbf{A}}, \mu_{\mathbf{b}, \mathbf{B}})) = \langle \mathbf{a}, \mathbf{b} \rangle + \text{Tr} \left(\mathbf{A}^{\frac{1}{2}} \mathbf{B} \mathbf{A}^{\frac{1}{2}} \right)^{\frac{1}{2}}$$

Note that $[\cdot, \cdot]_{\mathfrak{B}}$ is not an actual inner product since the Bures metric is not Hilbertian, unless we restrict ourselves to diagonal covariance matrices, in which case it is the inner product between $(\mathbf{a}, \sqrt{\mathbf{d}_{\mathbf{A}}})$ and $(\mathbf{b}, \sqrt{\mathbf{d}_{\mathbf{B}}})$. We use $[\mu_{\mathbf{a}, \mathbf{A}}, \mu_{\mathbf{b}, \mathbf{B}}]_{\mathfrak{B}}$ as a similarity measure which has, however, some regularity: one can show that when \mathbf{A} and \mathbf{B} are constrained to have equal traces and \mathbf{a}, \mathbf{b} equal norms, it is maximized when $\mathbf{a} = \mathbf{b}$ and $\mathbf{A} = \mathbf{B}$. Differentiating all three terms, its gradient w.r.t. \mathbf{A} simply reduces to $\nabla_{\mathbf{A}} [\mu_{\mathbf{a}, \mathbf{A}}, \mu_{\mathbf{b}, \mathbf{B}}]_{\mathfrak{B}} = \mathbf{T}^{\mathbf{AB}}$.

Computational Aspects The computational bottleneck of gradient-based Bures optimization lies in the matrix square roots and inverse square roots operations that arise when instantiating transport maps \mathbf{T} . The naive method using eigenvector decomposition is thus not satisfying, since it is far too time-consuming and that there is not yet, to the best of our knowledge, no straightforward way of performing it in batches on a GPU. We propose to use Newton-Schulz iterations (Algorithm 1, see [Higham, 2008], ch. 6) to approximate them. These iterations producing both a root and an inverse

root approximation, and, relying exclusively on matrix-matrix multiplications, stream efficiently on GPUs. Another problem lies in the numerous roots and inverse-roots that need to be approximated. To solve this, we exploit an alternative formula for $\mathbf{T}^{\mathbf{AB}}$ (proof in the supplementary material):

$$\mathbf{T}^{\mathbf{AB}} = \mathbf{A}^{-\frac{1}{2}} (\mathbf{A}^{\frac{1}{2}} \mathbf{B} \mathbf{A}^{\frac{1}{2}})^{\frac{1}{2}} \mathbf{A}^{-\frac{1}{2}} = \mathbf{B}^{\frac{1}{2}} (\mathbf{B}^{\frac{1}{2}} \mathbf{A} \mathbf{B}^{\frac{1}{2}})^{-\frac{1}{2}} \mathbf{B}^{\frac{1}{2}}. \quad (7)$$

In a gradient update, both the loss and the gradient of the metric are needed. In our case, we can use the matrix roots computed during loss evaluation and leverage the identity above to compute on a budget the gradients with respect to both scale matrices. Indeed, a naive computation of $\nabla_{\mathbf{A}} \mathfrak{B}^2(\mathbf{A}, \mathbf{B})$ and $\nabla_{\mathbf{B}} \mathfrak{B}^2(\mathbf{A}, \mathbf{B})$ would require the knowledge of 6 roots

$$\mathbf{A}^{\frac{1}{2}}, \mathbf{B}^{\frac{1}{2}}, (\mathbf{A}^{\frac{1}{2}} \mathbf{B} \mathbf{A}^{\frac{1}{2}})^{\frac{1}{2}}, (\mathbf{B}^{\frac{1}{2}} \mathbf{A} \mathbf{B}^{\frac{1}{2}})^{\frac{1}{2}}, \mathbf{A}^{-\frac{1}{2}}, \text{ and } \mathbf{B}^{-\frac{1}{2}} \text{ to compute transport maps}$$

$$\mathbf{T}^{\mathbf{AB}} = \mathbf{A}^{-\frac{1}{2}} (\mathbf{A}^{\frac{1}{2}} \mathbf{B} \mathbf{A}^{\frac{1}{2}})^{\frac{1}{2}} \mathbf{A}^{-\frac{1}{2}}, \mathbf{T}^{\mathbf{BA}} = \mathbf{B}^{-\frac{1}{2}} (\mathbf{B}^{\frac{1}{2}} \mathbf{A} \mathbf{B}^{\frac{1}{2}})^{\frac{1}{2}} \mathbf{B}^{-\frac{1}{2}},$$

namely four matrix roots and two matrix inverse roots. We can avoid computing those six matrices using identity (7) and limit ourselves to two runs of Algorithm 1, to obtain the same quantities as

$$\{\mathbf{Y}_1 \stackrel{\text{def}}{=} \mathbf{A}^{\frac{1}{2}}, \mathbf{Z}_1 \stackrel{\text{def}}{=} \mathbf{A}^{-\frac{1}{2}}\}, \{\mathbf{Y}_2 \stackrel{\text{def}}{=} (\mathbf{A}^{\frac{1}{2}} \mathbf{B} \mathbf{A}^{\frac{1}{2}})^{\frac{1}{2}}, \mathbf{Z}_2 \stackrel{\text{def}}{=} (\mathbf{A}^{\frac{1}{2}} \mathbf{B} \mathbf{A}^{\frac{1}{2}})^{-\frac{1}{2}}\} \\ \mathbf{T}^{\mathbf{AB}} = \mathbf{Z}_1 \mathbf{Y}_2 \mathbf{Z}_1, \mathbf{T}^{\mathbf{BA}} = \mathbf{Y}_1 \mathbf{Z}_2 \mathbf{Y}_1.$$

When computing the gradients of $n \times m$ $W_2(\alpha_i, \beta_j)$ in parallel, one only needs to run n Newton-Schulz algorithms (in parallel) to compute matrices $(\mathbf{Y}_1^i, \mathbf{Z}_1^i)_{i \leq n}$, and then $n \times m$ Newton-Schulz algorithms to recover cross matrices $\mathbf{Y}_2^{i,j}, \mathbf{Z}_2^{i,j}$. On the other hand, using an automatic differentiation framework would require to perform an additional backward computation of the same complexity as the forward evaluating computation of the roots and inverse roots, hence requiring roughly twice as many operations per batch.

Avoiding Rank deficiency at Optimization Time Although $\mathfrak{B}^2(\mathbf{A}, \mathbf{B})$ is defined for rank deficient matrices \mathbf{A} and \mathbf{B} , it is not differentiable with respect to these matrices if they are rank deficient. Indeed, as mentioned earlier, this can be compared to the non-differentiability of the Hellinger metric, $(\sqrt{x} - \sqrt{y})^2$ when x or y becomes null. If $\text{Im } \mathbf{B} \not\subset \text{Im } \mathbf{A}$, which is notably the case if $\text{rk } \mathbf{B} > \text{rk } \mathbf{A}$, then $\nabla_{\mathbf{A}} \mathfrak{B}^2(\mathbf{A}, \mathbf{B})$ no longer exists. However, even in that case, $\nabla_{\mathbf{B}} \mathfrak{B}^2(\mathbf{A}, \mathbf{B})$ exists iff $\text{Im } \mathbf{A} \subset \text{Im } \mathbf{B}$. Since it would be cumbersome to account for these subtleties in a large scale optimization setting, we propose to add a small common regularization term to all the factor products considered for our embeddings, and set $\mathbf{A}_\epsilon = \mathbf{L}\mathbf{L}^T + \epsilon \mathbf{I}$ where $\epsilon > 0$ is a hyperparameter. This ensures that all matrices are full rank, and thus that all gradients exist. Most importantly, all our derivations still hold with this regularization, and can be shown to leave the method to compute the gradients w.r.t \mathbf{L} unchanged, namely $(\mathbf{I} - \mathbf{T}^{\mathbf{A}_\epsilon \mathbf{B}}) \mathbf{L}$.

Algorithm 1 Newton-Schulz

Input: PSD matrix \mathbf{A} , $\epsilon > 0$

$\mathbf{Y} \leftarrow \frac{\mathbf{A}}{(1+\epsilon)\|\mathbf{A}\|}, \mathbf{Z} \leftarrow \mathbf{I}$

while not converged **do**

$\mathbf{T} \leftarrow (3\mathbf{I} - \mathbf{Z}\mathbf{Y})/2$

$\mathbf{Y} \leftarrow \mathbf{Y}\mathbf{T}$

$\mathbf{Z} \leftarrow \mathbf{T}\mathbf{Z}$

end while

$\mathbf{Y} \leftarrow \sqrt{(1+\epsilon)\|\mathbf{A}\|} \mathbf{Y}$

$\mathbf{Z} \leftarrow \frac{\mathbf{Z}}{\sqrt{(1+\epsilon)\|\mathbf{A}\|}}$

Output: square root \mathbf{Y} , inverse square root \mathbf{Z}

4 Experiments

We discuss in this section several applications of Elliptical embeddings. We first consider a simple mMDS type visualization task, in which elliptical distributions in $d = 2$ are used to embed isometrically points in high dimension. We argue that for such purposes, a more natural way to visualize ellipses is to use their precision matrix their covariances. This is due to the fact that the human eye somewhat acts in the opposite direction to the Bures metric, as discussed in Figure 3. We follow with more advanced experiments in which we consider the task of computing word embeddings on large corpora as a testing ground, and equal or improve on the state-of-the-art.

Visualizing Datasets Using Ellipsoids Multidimensional scaling [De Leeuw, 1977] aims at embedding points $\mathbf{x}_1, \dots, \mathbf{x}_n$ in a finite metric space in a lower dimensional one by minimizing the *stress* $\sum_{i,j} (\|\mathbf{x}_i - \mathbf{x}_j\| - \|\mathbf{y}_i, \mathbf{y}_j\|)^2$. In our case, this translates to the minimization of $\mathcal{L}_{\text{MDS}}(\mathbf{a}_1, \dots, \mathbf{a}_n, \mathbf{A}_1, \dots, \mathbf{A}_n) = \sum_{i,j} (\|\mathbf{x}_i - \mathbf{x}_j\| - W_2(\mu_{\mathbf{a}_i, \mathbf{A}_i}, \mu_{\mathbf{a}_j, \mathbf{A}_j}))^2$. This objective can be crudely minimized with a simple gradient descent approach operating on factors as advocated in Section 3, as illustrated in a toy example carried out using data from OECD's PISA study¹.

¹<http://pisadataexplorer.oecd.org/ide/idepisa/>

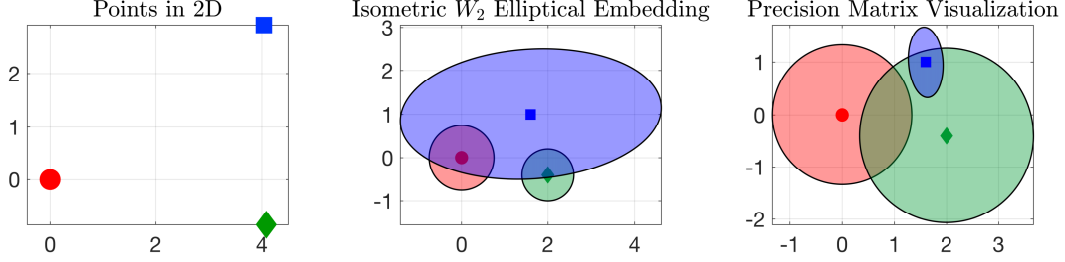


Figure 3: (left) three points on the plane. (middle) *isometric* elliptic embedding with the Bures metric: ellipses of a given color have the same respective distances as points on the left. Although the mechanics of optimal transport indicate that the blue ellipsoid is far from the two others, in agreement with the left plot, the human eye tends to focus on those areas that overlap (below the ellipsoid center) rather than those far away areas (north-east area) that contribute more significantly to the W_2 distance. (right) the precision matrix visualization, obtained by considering ellipses with the same axes but inverted eigenvalues, agree better with intuition, since they emphasize that overlap and extension of the ellipse means on the contrary that those axis contribute less to the increase of the metric.

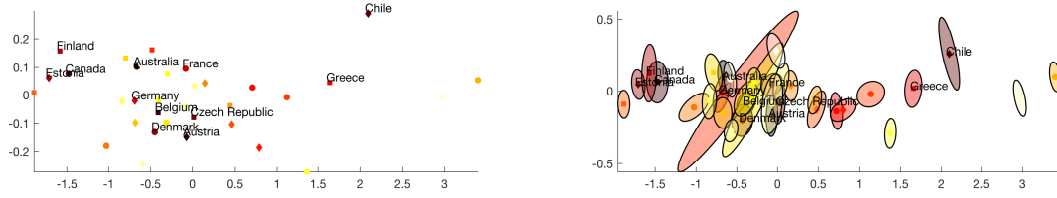


Figure 4: Toy experiment: visualization of a dataset of 10 PISA scores for 35 countries in the OECD. (left) MDS embeddings of these countries on the plane (right) elliptical embeddings on the plane using the precision visualization discussed in Figure 3. The initial normalized stress was 0.62, the stress with elliptical embeddings is close to $5e - 3$ after 1000 gradient iterations.

Word Embeddings The skipgram model [Mikolov et al., 2013a] computes word embeddings in a vector space by maximizing the log-probability of observing surrounding context words given an input central word. An extension to *diagonal* gaussian embeddings was proposed in [Vilnis and McCallum, 2015] using so-called energy based learning, which we further extend to elliptical distributions with *full* covariance matrices in the 2-Wasserstein space. Given a set \mathcal{R} of positive word/context pairs (w, c) and for each input word a set of negative contexts $\{c'_i \in N(w), i = 1, \dots, n\}$, we adapt Vilnis and McCallum’s loss function to the W_2^2 distance and minimize the following hinge loss

$$\sum_{(w,c) \in \mathcal{R}} \left[M - \left([\mu_w, \mu_c]_{\mathfrak{B}} - \frac{1}{n} \sum_{i=1}^n [\mu_w, \mu_{c'_i}]_{\mathfrak{B}} \right) \right]_+$$

where $M > 0$ is a margin parameter. We train our embeddings using adagrad [Duchi et al., 2011], sampling one negative context per positive context and, in order to prevent the norms of the embeddings to be too highly correlated with the corresponding word frequencies (see Figure in supplementary material), we use two distinct sets of embeddings for the input and context words. To generate batches, we use the same sampling tricks as in [Mikolov et al., 2013b], namely subsampling the frequent terms (using a threshold of 10^{-5} as recommended for large datasets) and smoothing the negative distribution by using probabilities $\{f_i^{3/4}/Z\}$ where f_i is the frequency of word i for sampling negative contexts $\{c'_i\}$. We compare our full elliptical to diagonal gaussian embeddings trained using the methods described [Vilnis and McCallum, 2015] on a collection of similarity datasets by computing the Spearman rank correlation between the similarity scores provided in the

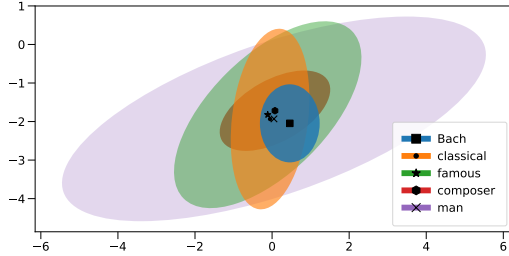


Figure 5: Precision matrix visualization of trained embeddings of a set of words on the plane spanned by the two principal eigenvectors of the covariance matrix of ‘Bach’, showing intuitive inclusion relations.

data and the scores we compute based on our embeddings. For fair comparison, we choose respective dimensions so that the number of free parameters is the same: because of the symmetry in the covariance matrix, elliptical embeddings in dimension d have $d + d(d + 1)/2$ free parameters (d for the means, $d(d + 1)/2$ for the covariance matrices), as compared with $2d$ for diagonal gaussians. For elliptical embeddings we use as a similarity measure a quantity we name *Bures cosine* which is, in analogy with the euclidean cosine, a renormalized version of the Bures product:

$$\cos_{\mathfrak{B}}[\rho_{\mathbf{a},\mathbf{A}}, \rho_{\mathbf{b},\mathbf{B}}] := \frac{\langle \mathbf{a}, \mathbf{b} \rangle}{\|\mathbf{a}\| \|\mathbf{b}\|} + \frac{\text{Tr}[\mathbf{A}^{\frac{1}{2}} \mathbf{B} \mathbf{A}^{\frac{1}{2}}]^{\frac{1}{2}}}{\sqrt{\text{Tr} \mathbf{A} \text{Tr} \mathbf{B}}}$$

Using this similarity measure rather than the Bures product is motivated by the fact that the norms of the embeddings are highly correlated with word frequencies (see Figure 6 in supplementary) and become dominant when comparing words with different frequencies scales. For this reason also we use context rather than input embeddings. We also evaluate our embeddings on the Entailment dataset ([Baroni et al., 2012]), on which we obtain results roughly comparable to those of [Vilnis and McCallum, 2015]. Note that in this framework, the asymmetry induced by training embeddings using the KL divergence actually gives an advantage as it is possible to fix the order of the arguments in the KL divergence, contrary to the similarity experiments.

Hypernymy In this experiment, we use the framework of [Nickel and Kiela, 2017] on hypernymy relationships to test our embeddings. A word A is said to be a *hypernym* of a word B if any B is a type of A , e.g. any *dog* is a type of *mammal*, thus constituting a tree-like structure on nouns. The WORDNET dataset [Miller, 1995] features a transitive closure of 743,241 hypernymy relations on 82,115 distinct nouns, which we consider as an undirected graph of relations \mathcal{R} on which we optimize the following loss:

$$\sum_{(u,v) \in \mathcal{R}, v' \in \mathcal{N}(u)} \mathcal{L}(u, v, \{v'\}) \text{ where } \mathcal{L}(u, v, \{v'\}) = \log e^{[\mu_u, \mu_v]_{\mathfrak{B}}} / (e^{[\mu_u, \mu_v]_{\mathfrak{B}}} + \sum_{v' \in \mathcal{N}(u)} e^{[\mu_u, \mu_{v'}]_{\mathfrak{B}}})$$

As with the skipgram model, for each noun u we sample a fixed number n of negative examples $v' \in \mathcal{N}(u)$. We train the model using RMSprop ([Tieleman and Hinton, 2015]) with, contrary to our skipgram experiments, only one set of embeddings. The embeddings are then evaluated on a link reconstruction task: we embed the full tree and rank the similarity of each positive hypernym pair (u, v) among all negative pairs (u, v') and compute the mean rank thus achieved as well as the mean average precision (MAP), using the Bures product as the similarity measure. Elliptical embeddings consistently outperform Poincare embeddings in high enough dimensions, as shown in Figure 6.

Conclusion We have proposed the space of elliptical distributions endowed with the W_2 metric to embed complex objects. This approach is numerically well grounded and provides a natural extension of point embeddings in \mathbb{R}^d . Future work

Table 1: Results for elliptical embeddings (evaluated using the Bures cosine) compared to diagonal Gaussian embeddings trained with the `seomoz` package (evaluated using cosine similarity as recommended by Vilnis and McCallum).

Dataset	W2G/45/C	Ell/12/BC
SimLex	33.28	24.09
WordSim	62.52	66.02
WordSim-R	69.37	71.07
WordSim-S	57.56	60.58
MEN	61.5	65.58
MC	79.5	65.95
RG	67.61	65.58
YP	20.86	25.14
MT-287	61.71	59.53
MT-771	58.11	56.78
RW	30.62	29.04

Table 2: Entailment benchmark: we evaluate our embeddings on the Entailment dataset using average precision (AP) and F1 score as metrics. For the F1 score we choose the optimal threshold at test time.

Model	AP	F1
W2G/45/Cosine	0.70	0.74
W2G/45/KL	0.72	0.74
Ell/12/Bures Cosine	0.70	0.73

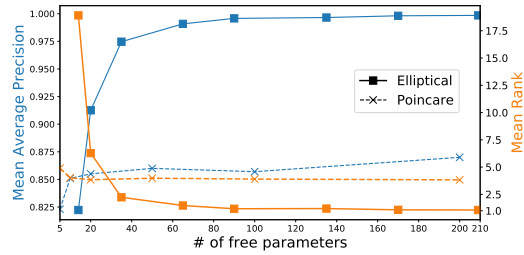


Figure 6: Reconstruction performance of our embeddings against Poincare embeddings (values reported from [Nickel and Kiela, 2017], we were not able to reproduce scores comparable to these values) evaluated by mean retrieved rank (lower=better) and MAP (higher=better).

will focus on the visualization possibilities offered by these embeddings, as well as more advanced constraints (such as inclusions or presences of interesections).

Acknowledgements MC acknowledges the support of a Chaire d’Excellence de l’Université Paris-Saclay.

References

- P-A Absil, Robert Mahony, and Rodolphe Sepulchre. *Optimization algorithms on matrix manifolds*. Princeton University Press, 2009.
- L. Ambrosio, N. Gigli, and G. Savaré. *Gradient flows in metric spaces and in the space of probability measures*. Springer, 2006.
- Ben Athiwaratkun and Andrew Gordon Wilson. Multimodal word distributions. *arXiv preprint arXiv:1704.08424*, 2017.
- Marco Baroni, Raffaella Bernardi, Ngoc-Quynh Do, and Chung-chieh Shan. Entailment above the word level in distributional semantics. In *Proceedings of the 13th Conference of the European Chapter of the Association for Computational Linguistics, EACL ’12*, pages 23–32. Association for Computational Linguistics, 2012.
- Rajendra Bhatia, Tanvi Jain, and Yongdo Lim. On the bures-wasserstein distance between positive definite matrices. *Expositiones Mathematicae*, 2018.
- Piotr Bojanowski, Edouard Grave, Armand Joulin, and Tomas Mikolov. Enriching word vectors with subword information. *arXiv preprint arXiv:1607.04606*, 2016.
- Ingwer Borg and Patrick JF Groenen. *Modern multidimensional scaling: Theory and applications*. Springer Science & Business Media, 2005.
- Jean Bourgain. On lipschitz embedding of finite metric spaces in hilbert space. *Israel Journal of Mathematics*, 52(1):46–52, 1985.
- Yann Brenier. Décomposition polaire et réarrangement monotone des champs de vecteurs. *CR Acad. Sci. Paris Sér. I Math*, 305(19):805–808, 1987.
- Alexander M Bronstein, Michael M Bronstein, and Ron Kimmel. Generalized multidimensional scaling: a framework for isometry-invariant partial surface matching. *Proceedings of the National Academy of Sciences*, 103(5):1168–1172, 2006.
- Elia Bruni, Nam Khanh Tran, and Marco Baroni. Multimodal distributional semantics. *J. Artif. Int. Res.*, 49(1):1–47, January 2014. ISSN 1076-9757.
- Mihai Bădoiu, Piotr Indyk, and Anastasios Sidiropoulos. Approximation algorithms for embedding general metrics into trees. In *Proceedings of the eighteenth annual ACM-SIAM symposium on Discrete algorithms*, pages 512–521. Society for Industrial and Applied Mathematics, 2007.
- Donald Bures. An extension of kakutani’s theorem on infinite product measures to the tensor product of semifinite w^* -algebras. *Transactions of the American Mathematical Society*, 135:199–212, 1969.
- Stamatis Cambanis, Steel Huang, and Gordon Simons. On the theory of elliptically contoured distributions. *Journal of Multivariate Analysis*, 11(3):368 – 385, 1981. ISSN 0047-259X. doi: [https://doi.org/10.1016/0047-259X\(81\)90082-8](https://doi.org/10.1016/0047-259X(81)90082-8). URL <http://www.sciencedirect.com/science/article/pii/0047259X81900828>.
- Jan De Leeuw. Applications of convex analysis to multidimensional scaling. In *Recent Developments in Statistics*, 1977.
- DC Dowson and BV Landau. The fréchet distance between multivariate normal distributions. *Journal of multivariate analysis*, 12(3):450–455, 1982.
- John Duchi, Elad Hazan, and Yoram Singer. Adaptive subgradient methods for online learning and stochastic optimization. *Journal of Machine Learning Research*, 12(Jul):2121–2159, 2011.

- Jittat Fakcharoenphol, Satish Rao, and Kunal Talwar. A tight bound on approximating arbitrary metrics by tree metrics. In *Proceedings of the thirty-fifth annual ACM symposium on Theory of computing*, pages 448–455. ACM, 2003.
- KT Fang, S Kotz, and KW Ng. *Symmetric Multivariate and Related Distributions*. Chapman and Hall/CRC, 1990.
- Lev Finkelstein, Evgeniy Gabrilovich, Yossi Matias, Ehud Rivlin, Zach Solan, Gadi Wolfman, and Eytan Ruppín. Placing search in context: the concept revisited. *ACM Trans. Inf. Syst.*, 20(1): 116–131, 2002.
- Matthias Gelbrich. On a formula for the l2 wasserstein metric between measures on euclidean and hilbert spaces. *Mathematische Nachrichten*, 147(1):185–203, 1990.
- Amir Globerson, Gal Chechik, Fernando Pereira, and Naftali Tishby. Euclidean embedding of co-occurrence data. *Journal of Machine Learning Research*, 8(Oct):2265–2295, 2007.
- Aditya Grover and Jure Leskovec. node2vec: Scalable feature learning for networks. In *Proceedings of the 22nd ACM SIGKDD international conference on Knowledge discovery and data mining*, pages 855–864. ACM, 2016.
- Guy Halawi, Gideon Dror, Evgeniy Gabrilovich, and Yehuda Koren. Large-scale learning of word relatedness with constraints. In *Proceedings of the 18th ACM SIGKDD International Conference on Knowledge Discovery and Data Mining*, KDD ’12, pages 1406–1414, New York, NY, USA, 2012. ACM.
- Nicholas J. Higham. *Functions of Matrices: Theory and Computation (Other Titles in Applied Mathematics)*. Society for Industrial and Applied Mathematics, Philadelphia, PA, USA, 2008.
- Felix Hill, Roi Reichart, and Anna Korhonen. Simlex-999: Evaluating semantic models with genuine similarity estimation. *Comput. Linguist.*, 41(4):665–695, December 2015. ISSN 0891-2017.
- Geoffrey E Hinton and Sam T Roweis. Stochastic neighbor embedding. In *Advances in neural information processing systems*, pages 857–864, 2003.
- Geoffrey E Hinton and Ruslan R Salakhutdinov. Reducing the dimensionality of data with neural networks. *science*, 313(5786):504–507, 2006.
- William B. Johnson and Joram Lindenstrauss. Extensions of Lipschitz mappings into a Hilbert space. In *Conference in modern analysis and probability (New Haven, Conn., 1982)*, volume 26 of *Contemp. Math.*, pages 189–206. Amer. Math. Soc., Providence, RI, 1984.
- Diederik P Kingma and Max Welling. Auto-encoding variational bayes. *arXiv preprint arXiv:1312.6114*, 2013.
- J.M. Lee. *Riemannian Manifolds: An Introduction to Curvature*. Graduate Texts in Mathematics. Springer New York, 1997.
- Laurens van der Maaten and Geoffrey Hinton. Visualizing data using t-sne. *Journal of Machine Learning Research*, 9(Nov):2579–2605, 2008.
- Luigi Malagò, Luigi Montrucchio, and Giovanni Pistone. Wasserstein-riemannian geometry of positive-definite matrices. *arXiv preprint arXiv:1801.09269*, 2018.
- Yariv Maron, Michael Lamar, and Elie Bienenstock. Sphere embedding: An application to part-of-speech induction. In *Advances in Neural Information Processing Systems*, pages 1567–1575, 2010.
- Tomas Mikolov, Kai Chen, Greg Corrado, and Jeffrey Dean. Efficient estimation of word representations in vector space. *CoRR*, 2013a.
- Tomas Mikolov, Ilya Sutskever, Kai Chen, Greg S Corrado, and Jeff Dean. Distributed representations of words and phrases and their compositionality. In *Advances in neural information processing systems*, pages 3111–3119, 2013b.

- George A. Miller. Wordnet: A lexical database for english. *Commun. ACM*, 38(11):39–41, November 1995.
- George A. Miller and Walter G. Charles. Contextual correlates of semantic similarity. *Language and Cognitive Processes*, 6(1):1–28, 1991.
- Maximillian Nickel and Douwe Kiela. Poincaré embeddings for learning hierarchical representations. In I. Guyon, U. V. Luxburg, S. Bengio, H. Wallach, R. Fergus, S. Vishwanathan, and R. Garnett, editors, *Advances in Neural Information Processing Systems 30*, pages 6341–6350. Curran Associates, Inc., 2017.
- Mohammad Norouzi, Tomas Mikolov, Samy Bengio, Yoram Singer, Jonathon Shlens, Andrea Frome, Greg Corrado, and Jeffrey Dean. Zero-shot learning by convex combination of semantic embeddings. In *International Conference on Learning Representations*, 2014. URL <http://arxiv.org/abs/1312.5650>.
- Jeffrey Pennington, Richard Socher, and Christopher Manning. Glove: Global vectors for word representation. In *Proceedings of the 2014 conference on empirical methods in natural language processing (EMNLP)*, pages 1532–1543, 2014.
- Gabriel Peyré and Marco Cuturi. Computational optimal transport. *arXiv preprint arXiv:1803.00567*, 2018.
- Kira Radinsky, Eugene Agichtein, Evgeniy Gabrilovich, and Shaul Markovitch. A word at a time: Computing word relatedness using temporal semantic analysis. In *Proceedings of the 20th International Conference on World Wide Web, WWW '11*, pages 337–346, New York, NY, USA, 2011. ACM.
- Sam T Roweis and Lawrence K Saul. Nonlinear dimensionality reduction by locally linear embedding. *science*, 290(5500):2323–2326, 2000.
- Herbert Rubenstein and John B. Goodenough. Contextual correlates of synonymy. *Commun. ACM*, 8(10):627–633, October 1965.
- Filippo Santambrogio. *Optimal Transport for Applied Mathematicians*. Birkhauser, 2015.
- Alex Smola, Arthur Gretton, Le Song, and Bernhard Schölkopf. *A Hilbert Space Embedding for Distributions*, pages 13–31. 2007.
- Joshua B Tenenbaum, Vin De Silva, and John C Langford. A global geometric framework for nonlinear dimensionality reduction. *science*, 290(5500):2319–2323, 2000.
- Minh thang Luong, Richard Socher, and Christopher D. Manning. Better word representations with recursive neural networks for morphology. In *In Proceedings of the Thirteenth Annual Conference on Natural Language Learning*. Tomas Mikolov, Wen-tau, 2013.
- T. Tieleman and G. Hinton. RMSprop Gradient Optimization. 2015.
- Nikolai G Ushakov. *Selected topics in characteristic functions*. Walter de Gruyter, 1999.
- Luke Vilnis and Andrew McCallum. Word representations via gaussian embedding. *Proceddings of the International Conference on Learning Representations (ICLR)*, 2015. arXiv preprint arXiv:1412.6623.
- K.Q. Weinberger and L.K. Saul. Distance metric learning for large margin nearest neighbor classification. *The Journal of Machine Learning Research*, 10:207–244, 2009.
- Dongqiang Yang and David M. W. Powers. Measuring semantic similarity in the taxonomy of wordnet. In *Proceedings of the Twenty-eighth Australasian Conference on Computer Science - Volume 38, ACSC '05*, pages 315–322, Darlinghurst, Australia, Australia, 2005. Australian Computer Society, Inc.

Supplementary Material

Equivalent formulations of $\mathbf{T}^{\mathbf{AB}}$

$\mathbf{T}^{\mathbf{AB}}$ is defined as the unique PSD matrix verifying $\mathbf{T}^{\mathbf{AB}} \mathbf{A} \mathbf{T}^{\mathbf{AB}} = \mathbf{B}$. Using this definition, we derive two equivalent formulations for $\mathbf{T}^{\mathbf{AB}}$:

$$\begin{aligned}\mathbf{T}^{\mathbf{AB}} &= \mathbf{A}^{-\frac{1}{2}} \left(\mathbf{A}^{\frac{1}{2}} \mathbf{B} \mathbf{A}^{\frac{1}{2}} \right)^{\frac{1}{2}} \mathbf{A}^{-\frac{1}{2}} \\ &= \mathbf{B}^{\frac{1}{2}} \left(\mathbf{B}^{\frac{1}{2}} \mathbf{A} \mathbf{B}^{\frac{1}{2}} \right)^{-\frac{1}{2}} \mathbf{B}^{\frac{1}{2}}\end{aligned}$$

The first is derived as in [Malagò et al., 2018]:

$$\begin{aligned}\mathbf{T}^{\mathbf{AB}} \mathbf{A} \mathbf{T}^{\mathbf{AB}} &= \mathbf{B} \\ \mathbf{A}^{\frac{1}{2}} \mathbf{T}^{\mathbf{AB}} \mathbf{A}^{\frac{1}{2}} \mathbf{A}^{\frac{1}{2}} \mathbf{T}^{\mathbf{AB}} \mathbf{A}^{\frac{1}{2}} &= \mathbf{A}^{\frac{1}{2}} \mathbf{B} \mathbf{A}^{\frac{1}{2}} \\ \mathbf{A}^{\frac{1}{2}} \mathbf{T}^{\mathbf{AB}} \mathbf{A}^{\frac{1}{2}} &= \left(\mathbf{A}^{\frac{1}{2}} \mathbf{B} \mathbf{A}^{\frac{1}{2}} \right)^{\frac{1}{2}} \\ \mathbf{T}^{\mathbf{AB}} &= \mathbf{A}^{-\frac{1}{2}} \left(\mathbf{A}^{\frac{1}{2}} \mathbf{B} \mathbf{A}^{\frac{1}{2}} \right)^{\frac{1}{2}} \mathbf{A}^{-\frac{1}{2}}\end{aligned}$$

We then adapt this derivation to obtain a second formulation of $\mathbf{T}^{\mathbf{AB}}$:

$$\begin{aligned}\mathbf{T}^{\mathbf{AB}} \mathbf{A} \mathbf{T}^{\mathbf{AB}} &= \mathbf{B} \\ (\mathbf{T}^{\mathbf{AB}})^{-1} \mathbf{B} (\mathbf{T}^{\mathbf{AB}})^{-1} &= \mathbf{A} \\ \mathbf{B}^{\frac{1}{2}} (\mathbf{T}^{\mathbf{AB}})^{-1} \mathbf{B}^{\frac{1}{2}} \mathbf{B}^{\frac{1}{2}} (\mathbf{T}^{\mathbf{AB}})^{-1} \mathbf{B}^{\frac{1}{2}} &= \mathbf{B}^{\frac{1}{2}} \mathbf{A} \mathbf{B}^{\frac{1}{2}} \\ \mathbf{B}^{\frac{1}{2}} (\mathbf{T}^{\mathbf{AB}})^{-1} \mathbf{B}^{\frac{1}{2}} &= \left(\mathbf{B}^{\frac{1}{2}} \mathbf{A} \mathbf{B}^{\frac{1}{2}} \right)^{\frac{1}{2}} \\ (\mathbf{T}^{\mathbf{AB}})^{-1} &= \mathbf{B}^{-\frac{1}{2}} \left(\mathbf{B}^{\frac{1}{2}} \mathbf{A} \mathbf{B}^{\frac{1}{2}} \right)^{\frac{1}{2}} \mathbf{B}^{-\frac{1}{2}} \\ \mathbf{T}^{\mathbf{AB}} &= \mathbf{B}^{\frac{1}{2}} \left(\mathbf{B}^{\frac{1}{2}} \mathbf{A} \mathbf{B}^{\frac{1}{2}} \right)^{-\frac{1}{2}} \mathbf{B}^{\frac{1}{2}}\end{aligned}$$

Derivation of the Riemannian gradient updates

From [Malagò et al., 2018], we have that the exp and log maps of the Riemannian Bures metric are given by:

$$\begin{aligned}\exp_{\mathbf{C}}(\mathbf{V}) &= (\mathcal{L}_{\mathbf{C}}(\mathbf{V}) + \mathbf{I}) \mathbf{C} (\mathcal{L}_{\mathbf{C}}(\mathbf{V}) + \mathbf{I}) \\ \log_{\mathbf{C}}(\mathbf{B}) &= (\mathbf{T}^{\mathbf{CB}} - \mathbf{I}) \mathbf{C} + \mathbf{C} (\mathbf{T}^{\mathbf{CB}} - \mathbf{I})\end{aligned}$$

where $\mathcal{L}_{\mathbf{C}}(\mathbf{V})$ is the solution of *Lyapunov* equation $\mathcal{L}_{\mathbf{C}}(\mathbf{V}) \mathbf{C} + \mathbf{C} \mathcal{L}_{\mathbf{C}}(\mathbf{V}) = \mathbf{V}$. One can show that the $\mathcal{L}_{\mathbf{C}}$ operator is linear, and that the following identity holds: $\mathcal{L}_{\mathbf{C}}(\mathbf{X} \mathbf{C} + \mathbf{C} \mathbf{X})$. In particular, $\mathcal{L}_{\mathbf{C}}(\log_{\mathbf{C}} \mathbf{B}) = \mathbf{T}^{\mathbf{CB}} - \mathbf{I}$.

From this, since $\text{grad}_{\mathbf{A}} \frac{1}{2} \mathfrak{B}^2(\mathbf{A}, \mathbf{B}) = -\log_{\mathbf{A}} \mathbf{B}$, the Riemannian gradient update is given by

$$\begin{aligned}\mathbf{A}_{t+1} &= \exp_{\mathbf{A}_t}(\eta_t \log_{\mathbf{A}_t} \mathbf{B}) \\ &= (\eta_t \mathcal{L}_{\mathbf{A}_t}(\log_{\mathbf{A}_t} \mathbf{B}) + \mathbf{I}) \mathbf{A}_t (\eta_t \mathcal{L}_{\mathbf{A}_t}(\log_{\mathbf{A}_t} \mathbf{B}) + \mathbf{I}) \\ &= ((1 - \eta_t)\mathbf{I} + \eta_t \mathbf{T}^{\mathbf{A}_t \mathbf{B}}) \mathbf{A}_t ((1 - \eta_t)\mathbf{I} + \eta_t \mathbf{T}^{\mathbf{A}_t \mathbf{B}})\end{aligned}$$

Derivation of the Euclidean gradient

Let $f(\mathbf{A}, \mathbf{B}) = \text{Tr}(\mathbf{B}^{\frac{1}{2}} \mathbf{A} \mathbf{B}^{\frac{1}{2}})^{\frac{1}{2}}$

Let us differentiate f w.r.t \mathbf{A} :

$$\begin{aligned}f(\mathbf{A} + \mathbf{H}, \mathbf{B}) &= \text{Tr} \left(\mathbf{B}^{\frac{1}{2}} (\mathbf{A} + \mathbf{H}) \mathbf{B}^{\frac{1}{2}} \right)^{\frac{1}{2}} \\ &= \text{Tr} \left(\mathbf{B}^{\frac{1}{2}} \mathbf{A} \mathbf{B}^{\frac{1}{2}} \left(\mathbf{I} + \left(\mathbf{B}^{\frac{1}{2}} \mathbf{A} \mathbf{B}^{\frac{1}{2}} \right)^{-1} \mathbf{B}^{\frac{1}{2}} \mathbf{H} \mathbf{B}^{\frac{1}{2}} \right) \right)^{\frac{1}{2}} \\ &= \text{Tr} \left(\mathbf{B}^{\frac{1}{2}} \mathbf{A} \mathbf{B}^{\frac{1}{2}} \left(\mathbf{I} + \frac{1}{2} \left(\mathbf{B}^{\frac{1}{2}} \mathbf{A} \mathbf{B}^{\frac{1}{2}} \right)^{-1} \mathbf{B}^{\frac{1}{2}} \mathbf{H} \mathbf{B}^{\frac{1}{2}} \right) \right) + O(\mathbf{H}^2) \\ &= f(\mathbf{A}, \mathbf{B}) + \frac{1}{2} \text{Tr} \left(\left(\mathbf{B}^{\frac{1}{2}} \mathbf{A} \mathbf{B}^{\frac{1}{2}} \right)^{-\frac{1}{2}} \mathbf{B}^{\frac{1}{2}} \mathbf{H} \mathbf{B}^{\frac{1}{2}} \right) + O(\mathbf{H}^2) \\ &= f(\mathbf{A}, \mathbf{B}) + \frac{1}{2} \langle \mathbf{B}^{\frac{1}{2}} \left(\mathbf{B}^{\frac{1}{2}} \mathbf{A} \mathbf{B}^{\frac{1}{2}} \right)^{-\frac{1}{2}} \mathbf{B}^{\frac{1}{2}}, \mathbf{H} \rangle + O(\mathbf{H}^2) \\ &= f(\mathbf{A}, \mathbf{B}) + \frac{1}{2} \langle \mathbf{T}^{\mathbf{A} \mathbf{B}}, \mathbf{H} \rangle + O(\mathbf{H}^2)\end{aligned}$$

where we used the fact that $(\mathbf{I} + \mathbf{H})^{\frac{1}{2}} = \mathbf{I} + \frac{1}{2} \mathbf{H} + O(\mathbf{H}^2)$.

Therefore $\nabla_{\mathbf{A}} f(\mathbf{A}, \mathbf{B}) = \frac{1}{2} \mathbf{T}^{\mathbf{A} \mathbf{B}}$

Let now $\mathbf{A} = \mathbf{L} \mathbf{L}^{\top}$, let us differentiate f w.r.t \mathbf{L}

$$\begin{aligned}
f\left((\mathbf{L} + \mathbf{H})(\mathbf{L} + \mathbf{H})^\top, \mathbf{B}\right) &= \text{Tr}\left(\mathbf{B}^{\frac{1}{2}}(\mathbf{A} + \mathbf{LH}^\top + \mathbf{L}^\top\mathbf{H} + \mathbf{HH}^\top)\mathbf{B}^{\frac{1}{2}}\right)^{\frac{1}{2}} \\
&= \text{Tr}\left(\mathbf{B}^{\frac{1}{2}}\mathbf{AB}^{\frac{1}{2}}\left(\mathbf{I} + \left(\mathbf{B}^{\frac{1}{2}}\mathbf{AB}^{\frac{1}{2}}\right)^{-1}\mathbf{B}^{\frac{1}{2}}(\mathbf{LH}^\top + \mathbf{HL}^\top + \mathbf{HH}^\top)\mathbf{B}^{\frac{1}{2}}\right)\right)^{\frac{1}{2}} \\
&= \text{Tr}\left(\mathbf{B}^{\frac{1}{2}}\mathbf{AB}^{\frac{1}{2}}\left(\mathbf{I} + \frac{1}{2}\left(\mathbf{B}^{\frac{1}{2}}\mathbf{AB}^{\frac{1}{2}}\right)^{-1}\mathbf{B}^{\frac{1}{2}}(\mathbf{LH}^\top + \mathbf{HL}^\top + \mathbf{HH}^\top)\mathbf{B}^{\frac{1}{2}}\right)\right) + O(\mathbf{H}^2) \\
&= f(\mathbf{A}, \mathbf{B}) + \text{Tr}\left(\left(\mathbf{B}^{\frac{1}{2}}\mathbf{AB}^{\frac{1}{2}}\right)^{-\frac{1}{2}}\mathbf{B}^{\frac{1}{2}}\mathbf{LH}^\top\mathbf{B}^{\frac{1}{2}}\right) + O(\mathbf{H}^2) \\
&= f(\mathbf{A}, \mathbf{B}) + \langle \mathbf{B}^{\frac{1}{2}}\left(\mathbf{B}^{\frac{1}{2}}\mathbf{AB}^{\frac{1}{2}}\right)^{-\frac{1}{2}}\mathbf{B}^{\frac{1}{2}}\mathbf{L}, \mathbf{H} \rangle + O(\mathbf{H}^2) \\
&= f(\mathbf{A}, \mathbf{B}) + \langle \mathbf{T}^{\mathbf{AB}}\mathbf{L}, \mathbf{H} \rangle + O(\mathbf{H}^2)
\end{aligned}$$

Therefore $\nabla_{\mathbf{L}}f(\mathbf{LL}^\top, \mathbf{B}) = \mathbf{T}^{\mathbf{AB}}\mathbf{L}$.

Using the same calculations, one can show that if $\mathbf{A} = \mathbf{LL}^\top + \varepsilon\mathbf{I}$, then we still have $\nabla_{\mathbf{L}}f(\mathbf{LL}^\top + \varepsilon\mathbf{I}, \mathbf{B}) = \mathbf{T}^{\mathbf{AB}}\mathbf{L}$:

$$\begin{aligned}
f\left((\mathbf{L} + \mathbf{H})(\mathbf{L} + \mathbf{H})^\top + \varepsilon\mathbf{I}, \mathbf{B}\right) &= \text{Tr}\left(\mathbf{B}^{\frac{1}{2}}(\mathbf{LL}^\top + \varepsilon\mathbf{I} + \mathbf{LH}^\top + \mathbf{L}^\top\mathbf{H} + \mathbf{HH}^\top)\mathbf{B}^{\frac{1}{2}}\right)^{\frac{1}{2}} \\
&= \text{Tr}\left(\mathbf{B}^{\frac{1}{2}}\mathbf{AB}^{\frac{1}{2}}\left(\mathbf{I} + \left(\mathbf{B}^{\frac{1}{2}}\mathbf{AB}^{\frac{1}{2}}\right)^{-1}\mathbf{B}^{\frac{1}{2}}(\mathbf{LH}^\top + \mathbf{HL}^\top + \mathbf{HH}^\top)\mathbf{B}^{\frac{1}{2}}\right)\right)^{\frac{1}{2}} \\
&= \text{Tr}\left(\mathbf{B}^{\frac{1}{2}}\mathbf{AB}^{\frac{1}{2}}\left(\mathbf{I} + \frac{1}{2}\left(\mathbf{B}^{\frac{1}{2}}\mathbf{AB}^{\frac{1}{2}}\right)^{-1}\mathbf{B}^{\frac{1}{2}}(\mathbf{LH}^\top + \mathbf{HL}^\top + \mathbf{HH}^\top)\mathbf{B}^{\frac{1}{2}}\right)\right) + O(\mathbf{H}^2) \\
&= f(\mathbf{A}, \mathbf{B}) + \text{Tr}\left(\left(\mathbf{B}^{\frac{1}{2}}\mathbf{AB}^{\frac{1}{2}}\right)^{-\frac{1}{2}}\mathbf{B}^{\frac{1}{2}}\mathbf{LH}^\top\mathbf{B}^{\frac{1}{2}}\right) + O(\mathbf{H}^2) \\
&= f(\mathbf{A}, \mathbf{B}) + \langle \mathbf{B}^{\frac{1}{2}}\left(\mathbf{B}^{\frac{1}{2}}\mathbf{AB}^{\frac{1}{2}}\right)^{-\frac{1}{2}}\mathbf{B}^{\frac{1}{2}}\mathbf{L}, \mathbf{H} \rangle + O(\mathbf{H}^2) \\
&= f(\mathbf{A}, \mathbf{B}) + \langle \mathbf{T}^{\mathbf{AB}}\mathbf{L}, \mathbf{H} \rangle + O(\mathbf{H}^2)
\end{aligned}$$

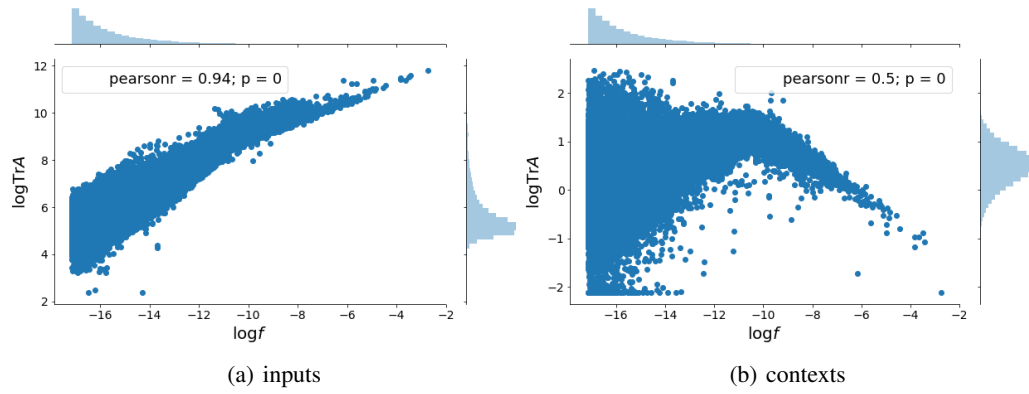


Figure 7: log-log plot of the traces of the embeddings' covariances vs. word frequency: the sizes of the input embeddings follow a power law, whereas context embeddings give less importance to very frequent words and emphasize on medium frequency words.